ISSN 0025-6544, Mechanics of Solids, 2016, Vol. 51, No. 2, pp. 206–215. © Allerton Press, Inc., 2016.
Original Russian Text © V.R. Bogdanov, G.T. Sulim, 2016, published in Izvestiya Akademii Nauk, Mekhanika Tverdogo Tela, 2016, No. 2, pp. 87–99.

Determination of the Material Fracture Toughness by Numerical Analysis of 3D Elastoplastic Dynamic Deformation

V. R. Bogdanov[1]* and G. T. Sulim[2]**

[1] *National Transport University, ul. Suvorova 1, Kiev, 01010 Ukraine*
[2] *Ivan Franko National University of L'viv, ul. Universytetskaya 1, Lviv, 79000 Ukraine*

Received December 6, 2013

Abstract—We develop a technique for calculating the plastic strain and fracture toughness fields of a material by solving dynamical 3D problems of determining the stress-strain state in the elastoplastic statement with possible unloading of the material taken into account. The numerical solution was obtained by a finite difference scheme applied to the three-point shock bending tests of parallelepiped-shaped bars made of different materials with plane crack-notches in the middle. The fracture toughness coefficient was determined for reactor steel. The numerically calculated stress tensor components, mean stresses, the Odquist parameter characterizing the accumulated plastic strain, and the fracture toughness are illustrated by graphs.

DOI: 10.3103/S0025654416020084

Keywords: *compact specimen, three-point bending, plastic strain, crack front, fracture toughness, dynamic problem, shock loading.*

1. INTRODUCTION

Problems of shock loading of deformable solids are currently topical and are used in very diverse settings. In [1], the plane elastic problem of dynamic interaction between an absolutely rigid indenter and an elastic isotropic homogeneous half-space at the supersonic stage of interaction was considered under the conditions of rigid adhesion of the contact surfaces. It was assumed that the contact region can be multiply connected. In [2], the action of nonstationary loading on the end surface of an elastic half-strip was studied. In [3], an experimental-computational technique for determining the dynamic stress intensity factor (DSIF) K_{I} was proposed. The critical fracture loads and the time of fracture of short compact specimens were determined experimentally. DSIF was calculated according to the linear theory as a convolution of the load and the unit signal-response, which was separately calculated by the finite element method. Rather complete studies of the dynamics of rigid-plastic structures were described in [4], where static and dynamic problems were studied in detail for rectangular, circular, and annular plates and membranes under the action of loading pulses of various shapes. There is an experimental technique [5] for studying the crack propagation and crack arrest in Charpy specimens under shock loading and in disk specimens under thermal shock action. The results of experimental and numerical modeling were used to determine the crack propagation rate in the specimens under study.

Numerical modeling of fracture processes allows one to optimize the program of actual tests of materials, significantly decrease the number of sometimes rather expensive experimental tests, and accelerate their completion. Fracture processes are modeled in the 2D [6–9] and 3D [10, 11] dynamic elastoplastic statements. In [8–10], the numerical modeling based on 2D equations of dynamics of elastoplastic materials with immovable cracks was used to determine the fracture toughness. In [12], an interesting attempt was made to develop the theory of solving initial boundary-value problems for bodies of revolution in the elastoplastic statement under thermal force loading. But this statement of the problem is constrained by the fact that the deformation process description is geometrically

* e-mail: vladislav_bogdanov@hotmail.com
** e-mail: sulym@franko.lviv.ua

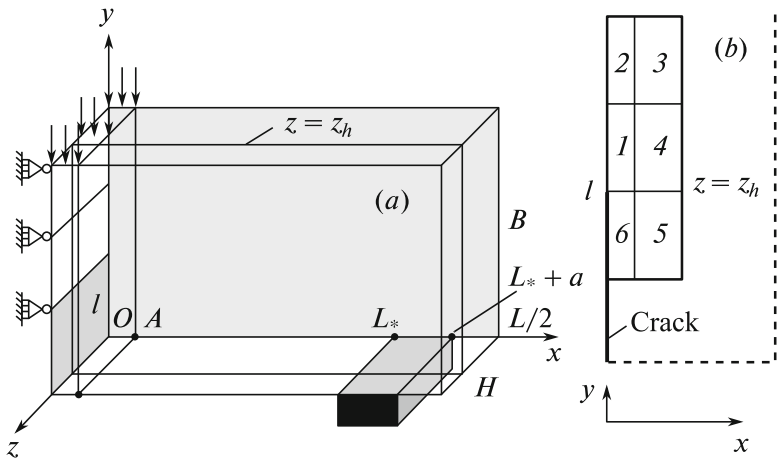

Fig. 1.

connected with the coordinate plane (the computational scheme of finite element method is used in spatial coordinates), which implies that small strains occur in trajectories of small curvature.

To determine the fracture toughness $K_{\mathrm{I}c}$ of a material experimentally, it is necessary to carry out a great deal of tests for numerous specimens, mainly in a sufficiently wide temperature range. Therefore, theoretical approaches that permit significantly decreasing the number of such tests are rather important. In [13], a probabilistic approach for determining the fracture toughness by using a quasistatic elastoplastic model is developed. A probabilistic approach for determining the fracture toughness, which permits determining it more precisely than by using the Master curve method, is similarly developed in [14]. The tests are carried out for a small number of specimens at normal temperature. The Weibull distribution parameters are nearly independent of the temperature and, only once determined, can be used to calculate the fracture toughness dependencies in a wide temperature range. In [15], an experimental method for determining the fracture toughness of ceramic materials on the basis of three-point bending tests of V-notched beam specimens was developed.

In [10] and in the present paper, it is shown that the developed method for solving 3D problems in the dynamic elastoplastic statement allows one to calculate the plastic strains more precisely than in [14], and hence determine the fracture toughness more adequately. Moreover, in this paper the stress-strain state of bars produced of reactor steel, titanium, aluminum, and silver and shaped as parallelepipeds with a plane saw-cut crack (a specimen with edge crack for determining the fracture toughness in three-point bending; i.e., SENB [16–19]) is determined by solving the spatial problem stated in the dynamic elastoplastic setting with the possible unloading of the material taken into account.

2. STATEMENT OF THE PROBLEM

Consider the deformation of an isotropic bar $\{|x| \le L/2,\ 0 \le y \le B,\ 0 \le z \le H\}$ of length L, height B, and thickness H whose cross-section is a rectangle $\Sigma = L \times B$ with saw-cut crack of length l along the vertical axis of the rectangle $\{x = 0,\ 0 \le y \le l,\ 0 \le z \le H\}$ in the middle. The bar contacts with two immovable supports in the domain $\{L_* \le |x| \le L_* + a,\ y = 0,\ 0 \le z \le H\}$. An absolutely rigid indenter falls on the bar from above, which contacts with the bar in the domain $\{|x| \le A,\ y = B,\ 0 \le z \le H\}$ during a short time interval. Its action is uniformly replaced by the normal load P which is uniformly distributed in time according to a linear law. Since the deformation problem is symmetric with respect to the plane $x = 0$, we consider only the right-hand side of the bar (Fig. 1 *a*). We assume that the contact domain does not change during the entire time interval.

Let $\mathbf{u} = (u_x, u_y, u_z)$ be the displacement vector related to the components of the small strain tensor ε_{ij} by the Cauchy formulas

$$\varepsilon_{ii} = \frac{\partial u_i}{\partial i}, \quad \varepsilon_{ij} = \frac{1}{2}\left(\frac{\partial u_i}{\partial j} + \frac{\partial u_j}{\partial i}\right) \quad (\Sigma_i;\ i, j = x, y, z). \tag{2.1}$$

We represent the boundary and initial conditions (under the assumption that the domain where the support reaction is applied and the contact between the specimen and the supports is smooth without

separation remains unchanged) in the form

$$\begin{aligned}
&x=0,\quad 0<y<l,\quad 0<z<H:\quad \sigma_{xx}=0,\quad \sigma_{xy}=0,\quad \sigma_{xz}=0,\\
&x=0,\quad 0<y<B,\quad 0<z<H:\quad u_x=0,\quad \sigma_{xy}=0,\quad \sigma_{xz}=0,\\
&x=L/2,\quad 0<y<B,\quad 0<z<H:\quad \sigma_{xx}=0,\quad \sigma_{xy}=0,\quad \sigma_{xz}=0,\\
&y=0,\quad 0<x<L_*,\quad 0<z<H:\quad \sigma_{yy}=0,\quad \sigma_{xy}=0,\quad \sigma_{yz}=0,\\
&y=0,\quad L_*<x<L_*+a,\quad 0<z<H:\quad u_y=0,\quad \sigma_{xy}=0,\quad \sigma_{yz}=0,\\
&y=0,\quad L_*+a<x<L/2,\quad 0<z<H:\quad \sigma_{yy}=0,\quad \sigma_{xy}=0,\quad \sigma_{yz}=0,\\
&y=B,\quad 0<x<A,\quad 0<z<H:\quad \sigma_{yy}=-P,\quad \sigma_{xy}=0,\quad \sigma_{yz}=0,\\
&y=B,\quad A<x<L/2,\quad 0<z<H:\quad \sigma_{yy}=0,\quad \sigma_{xy}=0,\quad \sigma_{yz}=0,\\
&z=0,\quad 0<x<L/2,\quad 0<y<B:\quad \sigma_{zz}=0,\quad \sigma_{xz}=0,\quad \sigma_{yz}=0,\\
&z=H,\quad 0<x<L/2,\quad 0<y<B:\quad \sigma_{zz}=0,\quad \sigma_{xz}=0,\quad \sigma_{yz}=0,\\
&t=0:\quad u_x=0,\quad u_y=0,\quad u_z=0,\quad \dot u_x=0,\quad \dot u_y=0,\quad \dot u_z=0.
\end{aligned}\tag{2.2}$$

where t is time and the dot above a symbol denotes the derivative with respect to time.

The dynamic relations in stresses have the form

$$\begin{aligned}
&\frac{\partial\sigma_{xx}}{\partial x}+\frac{\partial\sigma_{xy}}{\partial y}+\frac{\partial\sigma_{xz}}{\partial z}=\rho\frac{\partial^2u_x}{\partial t^2},\quad \frac{\partial\sigma_{xy}}{\partial x}+\frac{\partial\sigma_{yy}}{\partial y}+\frac{\partial\sigma_{yz}}{\partial z}=\rho\frac{\partial^2u_y}{\partial t^2},\\
&\frac{\partial\sigma_{xz}}{\partial x}+\frac{\partial\sigma_{yz}}{\partial y}+\frac{\partial\sigma_{zz}}{\partial z}=\rho\frac{\partial^2u_z}{\partial t^2}.
\end{aligned}\tag{2.3}$$

Here ρ is the density of the material.

For the physical model of the material we take a model based on the theory of nonisothermal plastic flow for a medium with strengthening and the Huber–Mises yield condition combined with the short-time creep hypothesis.

According to this model the stress-strain equations become

$$\varepsilon_{ij}=\varepsilon^e_{ij}+\varepsilon^p_{ij},\quad \varepsilon^e_{ij}=\frac{1}{2G}s_{ij}+\delta_{ij}(K_1\sigma+\varphi),\quad d\varepsilon^p_{ij}=s_{ij}\,d\lambda,\tag{2.4}$$

where $s_{ij}=\sigma_{ij}-\delta_{ij}\sigma$ is the stress tensor deviator, $\sigma=\frac{1}{3}(\sigma_{xx}+\sigma_{yy}+\sigma_{zz})$, δ_{ij} is the Kronecker symbol, G is the shear modulus, $K_1=1/(3K)$, $K=E/[3(1-2\nu)]$ is the bulk compression modulus relating the bulk extension 3ε, the mean stress σ, and the temperature elongation φ as $\varepsilon=K\sigma+\varphi$ (in this case, it is assumed that $\varphi\equiv 0$), ν is the Poisson ratio, E is the (Young) modulus of elasticity, and $d\lambda$ is a scalar function determined by the shape of the loading surface. We assume that this scalar function is a quadratic function of the stress deviator components s_{ij} and that

$$\begin{aligned}
&d\lambda=\left\{0\quad (f\equiv\sigma_i^2-\sigma_S^2(T)<0),\quad \frac{3d\varepsilon^p_i}{2\sigma_i}\quad (f=0,\ df=0)\right\},\quad d\varepsilon^p_{zz}=-d\varepsilon^p_{xx}-d\varepsilon^p_{yy},\\
&\sigma_i=\frac{1}{\sqrt{2}}[(\sigma_{xx}-\sigma_{yy})^2+(\sigma_{xx}-\sigma_{zz})^2+(\sigma_{yy}-\sigma_{zz})^2+6(\sigma^2_{xy}+\sigma^2_{xz}+\sigma^2_{yz})]^{1/2},\\
&d\varepsilon^p_i=\frac{\sqrt{2}}{3}\left\{(d\varepsilon^p_{xx}-d\varepsilon^p_{yy})^2+(d\varepsilon^p_{xx}-d\varepsilon^p_{zz})^2+(d\varepsilon^p_{yy}-d\varepsilon^p_{zz})^2+6[(d\varepsilon^p_{xy})^2+(d\varepsilon^p_{xz})^2+(d\varepsilon^p_{yz})^2]\right\}^{1/2},\\
&d\varepsilon_{ij}=d\left(\frac{\sigma_{ij}-\sigma}{2G}+K\sigma\right)+(\sigma_{ii}-\sigma)\,d\lambda\quad (i=j;\ i,j=x,y,z),\\
&d\varepsilon_{ij}=d\left(\frac{\sigma_{ij}}{2G}\right)+\sigma_{ij}\,d\lambda\quad (i\ne j;\ i,j=x,y,z),
\end{aligned}\tag{2.5}$$

where σ_i, ε^p_i, and $d\varepsilon^p_i$ are the stress intensity, the plastic strain intensity, and the increments of the latter.

We assume that the material strengthening is a result of the plastic strain according to the temperature dependence

$$\sigma_S(T) = \sigma_{02}(T)\left[1 + \frac{\kappa(T)}{\varepsilon_0}\right]^{\eta^*}, \quad \varepsilon_0 = \frac{\sigma_{02}(T_0)}{E}, \tag{2.6}$$

where T is temperature, $\kappa = \int \varepsilon_i^p$ is the Odquist parameter, $T_0 = 20^\circ$C, η^* is the strengthening coefficient, and $\sigma_S(T)$ is the yield point after the strengthening of the material at temperature T.

3. METHODS FOR SOLVING THE PROBLEM

We assume that the nonstationary interaction is studied on the time interval $[0, t_*]$. We take into account the nonstationary character of the loading P and numerically integrate over the time just as in the case of plane stress and deformed states [6, 7]. Here we apply the Gregory quadrature formula with equidistant nodes of order $m_1 = 3$ with coefficients D_n in the case of uniform digitation with respect to the time with nodes $t_k = k\Delta t \in [0, t_*]$ $(k = \overline{0, K})$. Then at time t_k with (2.4) taken into account we write

$$\varepsilon_{ii}^e = \frac{\sigma_{ii} - \sigma}{2G} + K\sigma, \quad \varepsilon_{ij}^e = \frac{\sigma_{ij}}{2G}, \quad \frac{d\varepsilon_{ii}^p}{dt} = (\sigma_{ii} - \sigma)\frac{d\lambda}{dt}, \quad \frac{d\varepsilon_{ij}^p}{dt} = \sigma_{ij}\frac{d\lambda}{dt} \quad (\textstyle\sum_i;\ i, j = x, y, z). \tag{3.1}$$

After the digitation, we write the strain increments as

$$\begin{aligned}
&\Delta\varepsilon_{xx,k} = B_1\sigma_{xx,k} + B_2(\sigma_{yy,k} + \sigma_{zz,k}) - b_{xx}, \quad \Delta\varepsilon_{xy,k} = B_3\sigma_{xy,k} - b_{xy},\\
&\Delta\varepsilon_{yy,k} = B_1\sigma_{yy,k} + B_2(\sigma_{xx,k} + \sigma_{zz,k}) - b_{yy}, \quad \Delta\varepsilon_{xz,k} = B_3\sigma_{xz,k} - b_{xz},\\
&\Delta\varepsilon_{zz,k} = B_1\sigma_{zz,k} + B_2(\sigma_{xx,k} + \sigma_{yy,k}) - b_{zz}, \quad \Delta\varepsilon_{yz,k} = B_3\sigma_{yz,k} - b_{yz},\\
&B_1 = \frac{1}{3}\left(K + \frac{1}{G} + 2D_0\Delta\lambda_k\right), \quad B_2 = \frac{1}{3}\left(K - \frac{1}{G} - D_0\Delta\lambda_k\right), \quad B_3 = \frac{1}{2G} + D_0\Delta\lambda_k,\\
&b_{ij} = \frac{1}{2G}\sigma_{ij,k-1} + \delta_{ij}\left(K - \frac{1}{2G}\right)\sigma_{k-1} - \sum_{n=1}^{m} D_n(\sigma_{ij,k-n} + \delta_{ij}\sigma_{k-n})\Delta\lambda_{k-n} \quad (i, j = x, y, z).
\end{aligned} \tag{3.2}$$

The function $\psi = 1/(2G) + \Delta\lambda$, which characterizes the yield condition, with (2.5) taken into account, can be written as

$$\begin{aligned}
&\psi = \left\{\frac{1}{2G} \ \ (f < 0), \quad \frac{1}{2G} + \frac{3\Delta\varepsilon_i^p}{2\sigma_i} \ \ (f = 0,\ df = 0)\right\},\\
&\Delta\varepsilon_i^p = \frac{\sqrt{2}}{3}\big\{(\Delta\varepsilon_{xx}^p - \Delta\varepsilon_{yy}^p)^2 + (\Delta\varepsilon_{xx}^p - \Delta\varepsilon_{zz}^p)^2 + (\Delta\varepsilon_{yy}^p - \Delta\varepsilon_{zz}^p)^2\\
&\qquad + 6[(\Delta\varepsilon_{xy}^p)^2 + (\Delta\varepsilon_{xz}^p)^2 + (\Delta\varepsilon_{yz}^p)^2]\big\}^{1/2},\\
&\Delta\varepsilon_{ij,k}^e = \frac{1}{2G}\Delta\sigma_{ij,k} + \delta_{ij}\left(K - \frac{1}{2G}\right)\Delta\sigma_k, \quad \Delta\varepsilon_{ij}^p = \Delta\varepsilon_{ij} - \Delta\varepsilon_{ij}^e \quad (i, j = x, y, z).
\end{aligned} \tag{3.3}$$

To take into account the plastic strains contained in conditions (3.3), we use the successive approximation method and can therefore reduce solving the elastoplastic problem to solving the sequence of linear problems

$$\begin{aligned}
&\psi^{(n+1)} = \left\{\psi^{(n)}p + \frac{1-p}{2G} \ \ (Q_\sigma < -Q), \quad \psi^{(n)} \ \ (|Q_\sigma| < -Q), \quad \psi^{(n)}\frac{\sigma_i^{(n)}}{\sigma_S(T)} \ \ (Q_\sigma > Q)\right\},\\
&Q_\sigma = \sigma_i^{(n)} - \sigma_S(T), \quad 0 \le p \le 1.
\end{aligned} \tag{3.4}$$

(Her Q is the value of the largest deviation of the stress intensity from the yield point).

From system (3.2), we obtain the following expressions for the stresses:

$$\sigma_{xx,k} = A_1\Delta\varepsilon_{xx,k} + A_2\Delta\varepsilon_{yy,k} + A_2\Delta\varepsilon_{zz,k} + Y_{xx}, \quad \sigma_{xy,k} = A_3\Delta\varepsilon_{xy,k} + Y_{xy},$$
$$\sigma_{yy,k} = A_2\Delta\varepsilon_{xx,k} + A_1\Delta\varepsilon_{yy,k} + A_2\Delta\varepsilon_{zz,k} + Y_{yy}, \quad \sigma_{xz,k} = A_3\Delta\varepsilon_{xz,k} + Y_{xz},$$
$$\sigma_{zz,k} = A_2\Delta\varepsilon_{xx,k} + A_2\Delta\varepsilon_{yy,k} + A_1\Delta\varepsilon_{zz,k} + Y_{zz}, \quad \sigma_{yz,k} = A_3\Delta\varepsilon_{yz,k} + Y_{yz},$$
$$Y_{xx} = A_1 b_{xx} + A_2 b_{yy} + A_2 b_{zz}, \quad Y_{xy} = A_3 b_{xy}, \quad A_1 = \frac{B_1 + B_2}{(B_1 - B_2)(B_1 + 2B_2)}, \tag{3.5}$$
$$Y_{yy} = A_2 b_{xx} + A_1 b_{yy} + A_2 b_{zz}, \quad Y_{xz} = A_3 b_{xz}, \quad A_2 = -\frac{B_2}{(B_1 - B_2)(B_1 + 2B_2)},$$
$$Y_{zz} = A_2 b_{xx} + A_2 b_{yy} + A_1 b_{zz}, \quad Y_{yz} = A_3 b_{yz}, \quad A_3 = -1B_3.$$

The increment $\Delta\mathbf{u}$ of the displacement vector is related to the strain increment as follows:

$$\Delta\varepsilon_{ii} = \frac{\partial\Delta u_i}{\partial t}, \quad \Delta\varepsilon_{ij} = \frac{1}{2}\left(\frac{\partial\Delta u_i}{\partial j} + \frac{\partial\Delta u_j}{\partial i}\right) \quad (\Sigma_i;\ i,j = x,y,z). \tag{3.6}$$

An independent parameter characterizing the loading process is the time t (its discrete analog). But to describe the variations in some characteristics, for the independent parameter (variable) we take the calculated value of the stress intensity factor K_{I} (SIF) near the crack in the static problem of three-point bending by the force F of an elastically deformed SENB specimen. We determine the corresponding values of this "elastic SIF" at each time t_k by the relation (see [20; p. 360])

$$K_{\mathrm{I}} = 12F\frac{\sqrt{l}}{BH}\left[1.93 - 3.07\frac{l}{B} + 14.53\left(\frac{l}{B}\right)^2 - 25.11\left(\frac{l}{B}\right)^3 + 25.8\left(\frac{l}{B}\right)^4\right], \tag{3.7}$$

where $F = 2APH$ is the contact force ($P = p_{01} + p_{02}k$) and $4B$ is the distance between the supports.

The calculations were carried out for reactor steel 15Kh2NMFA, titanium, aluminum, and silver.

4. DETERMINATION OF THE FRACTURE TOUGHNESS

In [21], the critical brittle fracture stresses $S_C(k)$ for reactor steels were experimentally determined using the data of uniaxial extension with the subsequent fracture. On the basis of these results, we proposed to approximate the yield point $\sigma_{02}(T)$ and the critical brittle fracture stresses as follows:

$$\sigma_{02}(T) = a - c(T + 273) + b\exp[-h(T + 273)], \tag{4.1}$$
$$S_C(\kappa) = [C_1 + C_2\exp(-A_d\kappa)]^{-1/2}, \tag{4.2}$$

where the parameters a, c, b, h, C_1, C_2, and A_d characterize the mechanical properties of the polycrystalline material. To determine the fracture toughness factor $K_{\mathrm{I}c}$ and describe the dynamic processes in the specimens made of a polycrystalline material with carbide inclusions (which are metals), the numerical simulation of the stress-strain state of the specimen in the three-point bending test was used in the spatial dynamic elastoplastic setting. This setting was supplemented with the brittle fracture criterion for the polycrystalline material, and the Weibull distribution function was used. The attained plastic strains and stresses were determined by the finite difference method with variable step along the axes Ox (N_1 elements), Uy (N_2 elements), and Oz (N_3 elements). In this case, the local brittle fracture criterion was used for each three-dimensional elementary grid cell in the form [14, 21]

$$\sigma_{1,k} + m_{T\varepsilon,k}(T, \kappa_k(T))\sigma_{\mathrm{eff},k} \geq \sigma_d, \tag{4.3}$$
$$\sigma_{1,k} \geq S_C(\kappa_k(T)), \tag{4.4}$$
$$\sigma_{\mathrm{eff},k} = \sigma_{i,k} - \sigma_{02}, \tag{4.5}$$

where σ_1 is the maximum principal stress, σ_i is the stress intensity, σ_d is the effective strength of carbides and other particles on which the cleavage microcracks originate, and σ_{eff} is the effective stress. Since the main contribution to the appearance of plastic strains is due to the shear stress, it is expedient to use the expression $\sigma_{\mathrm{eff}} = \sigma_i - \tau_{02}$ as σ_{eff}. Therefore, with regard to the data experimentally determined in [14, 21], here we use its discrete analog (4.5).

Table 1

Metal	Reactor steel	Titanium	Aluminum	Silver
G_k	0.535714	0.409091	0.358209	0.284672
E kg/m^2	2.15×10^{10}	1.12×10^{10}	0.7×10^{10}	0.8×10^{10}
ν	0.272727	0.22	0.34	0.37
ρ kg/m^3	7700	4505	2688.9	1050

The strengthening coefficient $m_{T\varepsilon}$ depending on the temperature T and the attained plastic strain ε can be written as the product of the temperature $m_T(T)$ by the strain component $m_\varepsilon(\kappa)$ [14],

$$m_{T\varepsilon}(T, \kappa_k) = m_T(T) m_\varepsilon(\kappa_k). \tag{4.6}$$

Here $m_T(T) = \sigma_{Ys}(T)$, $m_\varepsilon(\kappa_k) = S_0/S_C(\kappa_k)$, $S_0 \equiv S_C(\kappa)\big|_{\kappa=0}$, and σ_{Ys} is the temperature-dependent component of the yield point. In [14], the relation $m_T(T) = m_0 \sigma_{Ys}(T)$ was used with weight constant m_0 experimentally determined at level 0.1. But here we propose to proceed without additional experiments and estimate $m_T(T)$ directly by $\sigma_{Ys}(T)$; i.e., we in fact a priori assume that $m_0 = 1$.

To take into account the fact that the fracture is a probability process owing to the carbide inclusions, we assume that σ_d is a probability parameter obeying the Weibull distribution function [8–10, 13, 14] with parameters η, σ_{d0}, and $\tilde{\sigma}_d$,

$$p(\sigma_d) = 1 - \exp\left[-\left(\frac{\sigma_d - \sigma_{d0}}{\tilde{\sigma}_d}\right)^\eta\right]. \tag{4.7}$$

Since the fracture in each grid cell is assumed to be an independent event for given T_0 and K_0, the probability of the brittle fracture for a given value of $P_f(K_\mathrm{I})$ is calculated by the formula [8–10, 13, 14]:

$$P_f(K_\mathrm{I})\big|_{T=T_0} = 1 - \exp\left[-\frac{1}{(\tilde{\sigma}_d)^\eta} \sum_{l=1}^{K} \tilde{\omega}_l \sum_{m=1}^{M} \sum_{n=1}^{N} (\sigma_{\mathrm{nuc}}^{l,n,m} - \sigma_{d0})^\eta\right], \tag{4.8}$$

where $\sigma_{\mathrm{nuc}}^{l,n,m} = \sigma_1^{l,n,m} + m_T^{l,n,m} m_\varepsilon^{l,n,m} \sigma_{\mathrm{eff}}^{l,n,m}$, $\tilde{\omega}_l = 2h_l/\rho_{\mathrm{uc}}$, h_l is the step of the grid in the computation domain along the axis Oz, l, m, and n are the indices of elementary cells formed by the grids along the axes Ox, Oy, and Oz, respectively, and ρ_{uc} is the mean size of the metal grain. And in the sums in (4.8), we take into account only the cells which are destroyed according to the conditions

$$\sigma_{\mathrm{eff}}^{l,n,m} \geq 0, \quad \sigma_1 \geq S_C, \quad \sigma_{\mathrm{nuc}}^{l,n,m} \geq \sigma_{d0}^{l,n,m}. \tag{4.9}$$

5. NUMERICAL REALIZATION

The values of the elasticity modulus, Poisson's ratio, density, and ratio $G_K = G/K$ of the shear modulus to the bulk compression modulus of the materials under study are presented in Table 1. The interval between the points of digitation of the computation domain is the least near the crack tip and on the boundaries of the computation domain. The typical dimension of the cells at the distance at most equal to 0.4 mm from the crack tip is set to be equal to the mean size of the metal grain $\rho_{\mathrm{uc}} = 0.05$ mm. The digitation with respect to time is uniform. The use of the finite difference method is justified in [22].

Figures 2–3 illustrate the results of calculations obtained for specimens of length $L = 60$ mm, height $B = 10$ mm, width $H = 50$ mm; the depth of the notch at the specimen center is $l = 3$ mm, and the strengthening coefficient is $\eta^* = 0.05$. The distance between the reference points is 40 mm. The time step is $\Delta t = 0.0005$ s. Half the length of the contact region is $A = 2.5$ mm, $N_1 = 22$, $N_2 = 22$, $N_3 = 21$, the coefficients are $p_{01} = 8$ MPa and $p_{02} = 10$ MPa, and the temperature is $T = 50°$C.

It was indicated in [3] that the specimens were destroyed in 21–23 ms after the collision of the bodies. To verify the approach proposed here, the process of fracture of specimens of material and size the same as in [3] and under the same contact loading was modeled in the dynamical elastoplastic statement with regard to the material unloading and the crack length extension according to the local brittle fracture criterion (4.9). The calculations showed that the specimens were completely destroyed in 23 ms. This, to some extent, confirms that the problem is well posed and the developed model is adequate.

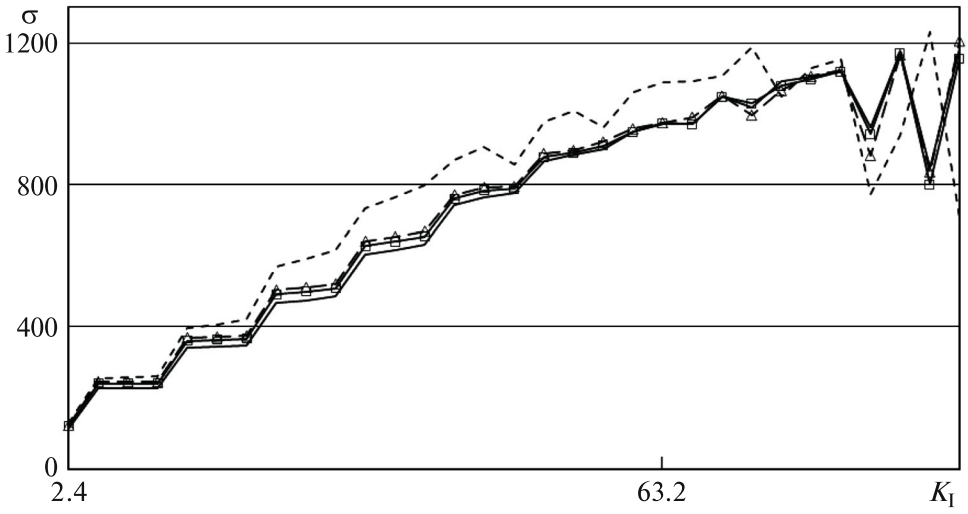

Fig. 2.

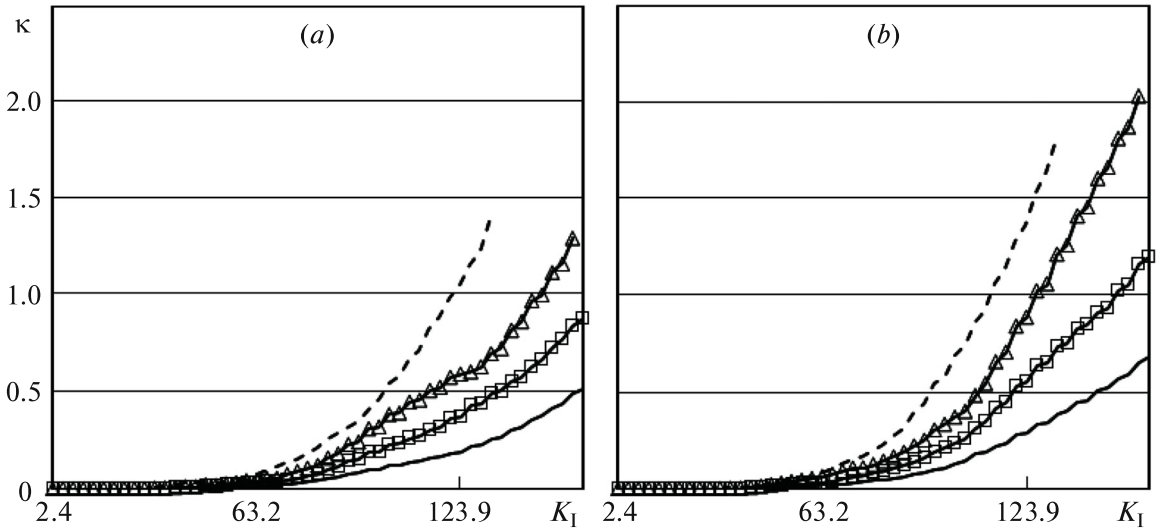

Fig. 3.

Figures 2–4 illustrate the results of computations for metals with the possible unloading of the material. The unloading occurs by the following algorithm. If, in a cell, the absolute value of the stress becomes less than the maximal value attained previously, then it is assumed that the plastic strains cease to increase. the material ceases to strengthen, and the stresses again linearly depend on the strains. The plastic strains again begin to increase and the material continues to strengthen when the absolute value of stresses exceeds the maximal value attained previously.

Figure 2 presents the graphs of mean stresses σ (MPa) arising near the crack tip in the three-dimensional compact specimen in the plane $z = 41.3$ mm (in the interior of cell *1* in Fig. 1 *b*). The solid, solid with square markers, dashed with triangular markers, and dashed lines correspond to the computations for the reactor steel, titanium, aluminum, and silver, respectively. While the "elastic SIF" is less than $K_I = K_I^* = 82.3\,\text{MPa}\sqrt{\text{m}}$, the calculated mean stresses σ increase as the coefficient G_K decreases, and the dependence on K_I is practically monotone. But as the SIF K_I exceeds the value K_I^*, the monotone character disappears and the mean stresses begin to oscillate.

We do not present the graphic dependencies of σ on K_I for the cross-section $z = 49.88$ mm, but we note that the oscillations begin in this cross-section when the elastic SIF attains the

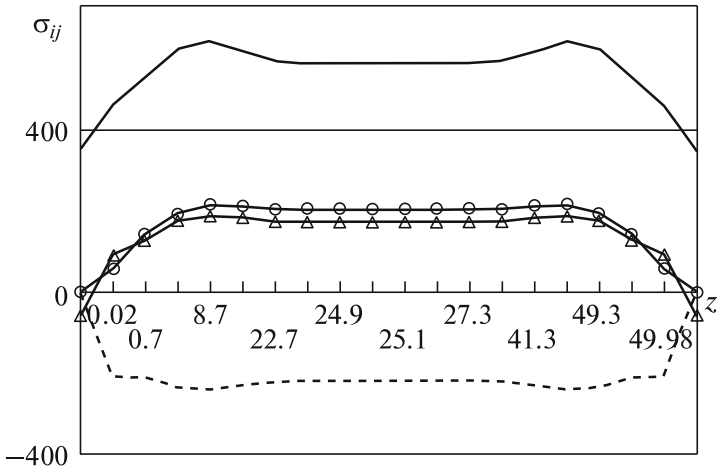

Fig. 4.

value $K_{\mathrm{I}} = 54\,\mathrm{MPa}\sqrt{\mathrm{m}}$, and the level of mean stresses σ is then by 23% less than that in the plane $z = 41.3$ mm.

Figure 3 shows the graphs of the Odquist parameter characterizing the plastic strain accumulated in cell *1* ahead of the crack front for the reactor steel, titanium, aluminum, and silver (solid, solid with square markers, solid with triangular markers, and dashed lines, respectively). By analyzing Fig. 3, one can see that the smaller the ratio of the shear modulus to the bulk compression modulus G_K, the greater the Odquist parameter and hence the plastic strain accumulated ahead of the crack front.

By comparing the plastic strains in the cross-sections $z = 41.3$ mm (Fig. 1 *a*) and $z = 39.88$ mm (Fig. 1 *b*), one can see that the plastic strains in the cross-sections located nearer to the lateral surfaces of the specimen is greater than in the middle.

While the elastic SIF K_{I} take values in the interval [84.4, 102.6] for reactor steel, [84.4, 105.7] for titanium, [84.4, 108.7] for aluminum, and [84.4, 87.4] for silver, respectively, the spread of the Odquist parameter values in the considered cross-sections $z = 4.3$ and $z = 49.88$ does not exceed 6%. As the loading process is complete, their greatest deviation attains the values 35%, 33%, 42%, and 25%, respectively.

Figure 4 presents the graphs of stress distribution over the thickness of a three-dimensional specimen in three-point bending near the crack front (cells in row *1* in Fig. 1 *b*) when the stress intensity attains the value $K_{\mathrm{I}} = 36.7\,\mathrm{MPa}\sqrt{\mathrm{m}}$. The solid, solid with square markers, solid with circular markers, and dashed lines correspond to the stresses σ_{xx}, σ_{yy}, σ_{zz}, and σ_{xy}.

To compare the obtained results with the results obtained in [14], the results of computations without the material unloading taken into account are given in Figs. 5–7. Figures 6 and 7 present the graphs of the mean stress and the Odquist parameter versus the temperature near the crack tip (cells *1*, Fig. 1 *b*), respectively. Here the solid with square markers, solid, and solid with circular markers lines correspond to the values in the planes $z = 32.3$, 41.3, and 48.3 mm, respectively. These dependencies are compared with the results of calculations for the plane strain state (dashed lines). As the temperature increases, the predicted increase in the accumulated plastic strain is also observed.

The probability curves $K_{\mathrm{I}c}(T)$ (solid lines in Fig. 7) are constructed for radiated specimens (produced of steel 15Kh2NMFA) of thickness 50 mm in the embrittled state. Lines *1*, *2*, *3* correspond to the values of the probability $P_f(K_{\mathrm{I}})$ of brittle fracture at the levels 0.05, 0.5, 0.95 and are compared with similar curves in [14] (dashed lines). They were calculated for the parameter m_T in the form [14]

$$m_T = \sigma_{02}(T_0) - \sigma_{02}(350^\circ\mathrm{C})).$$

The temperature dependence of the yield point (4.1) for steel in the embrittled state was constructed for [14] $a = 867$ MPa, $b = 975$ MPa, $c = 0.305\,\mathrm{MPa\,K^{-1}}$, and $h = 1.04 \times 10^{-2}\,\mathrm{K^{-1}}$. The parameters of the Weibull distribution (4.8) were determined for the following value of the critical SIF (fracture toughness) [14]: $K_{\mathrm{I}c}(50^\circ\mathrm{C})\big|_{P_f=0.05} = 53$, $K_{\mathrm{I}c}(50^\circ\mathrm{C})\big|_{P_f=0.5} = 88$, and $K_{\mathrm{I}c}(50^\circ\mathrm{C})\big|_{P_f=0.95} = 123$ taken from the dashed lines in Fig. 7 at the temperature 50°C.

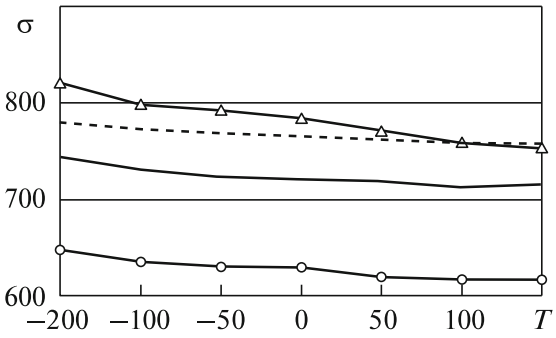

Fig. 5.

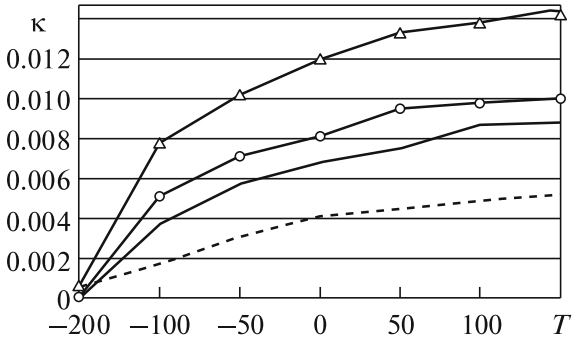

Fig. 6.

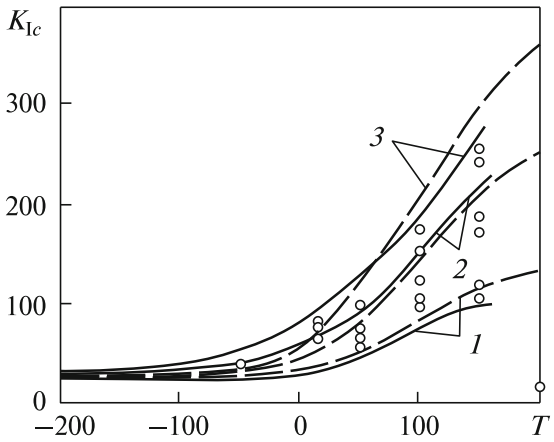

Fig. 7.

The minimum of the root-mean-square deviation

$$\min\{[P_f(K_\mathrm{I})|_{K_\mathrm{I}=53,\ T=50^\circ\mathrm{C}}-0.05]^2+[P_f(K_\mathrm{I})|_{K_\mathrm{I}=88,\ T=50^\circ\mathrm{C}}-0.5]^2+[P_f(K_\mathrm{I})|_{K_\mathrm{I}=123,\ T=50^\circ\mathrm{C}}-0.95]^2\}$$

was used to calculated the Weibull parameters $\tilde{\sigma}_d = 16840$ MPa, $\eta = 7$, and $\sigma_{d0} = 1793$ MPa (in [14], they were equal to $\tilde{\sigma}_d = 4103$ MPa, $\eta = 12$, and $\sigma_{d0} = 1840$ MPa).

To calculate the values of the function $P_f(K_\mathrm{I})$ from the dependence (4.8), the problems were solved for the temperature T_0 in the range from -200°C to 2006∘C with a step of 50°C. The values of the stress intensity K_I corresponding to the brittle fracture probability values 0.05, 0.5, and 0.95 were taken, and the points obtained on the plane TOK_I (Fig. 7) were used to construct the desired dependencies for the fracture toughness $K_{Ic}(T)$.

The solid lines in Fig. 7 present the curves of the fracture toughness $K_{Ic}(T)$ for the embrittled steel specimens of thickness 50 mm calculated by the expression (4.5) in contrast to [14]. The resulting fracture toughness curves $K_{Ic}(T)$ for the embrittled reactor steel (solid lines) completely cover the experimental results [14] indicated in Fig. 7 by circular markers.

6. CONCLUSION

A technique for determining 3D plastic strain fields by solving the 3D problems numerically in the dynamic elastoplastic statement is developed. The solutions of the 3D problem of plastic strain accumulation in a specimen, which permit determining the fracture toughness in the three-point bending in the dynamical elastoplastic setting with the material unloading process for four different materials taken into account, are used to show that the smaller the ratio of the shear modulus to the bulk compression modulus, the greater the plastic strains are. The obtained results describe the fracture process more precisely than the solutions of the quasistatic elastoplastic problems in the 2D and 3D statements used for this purpose. This allows one to improve the technique for determining the fracture toughness of materials numerically, which was proposed in [14], and obtain adequate models of plastic strain development and stress concentration near the crack front.

REFERENCES

1. A. L. Medvedskii and D. V. Tarlakovskii, "Nonstationary Contact between a Nondeformable Punch with Imperfections and an Elastic Half-Plane on the Segment of Supersonic Penetration," Vestnik MAI **18** (6), 125–132 (2011).
2. V. D. Kubenko, V. V. Gavrilenko, and D. V. Tarlakovskii, "Action of Nonstationary Load on the Surface of an Elastic Strip," Dopov. Nat. Akad. Nauk Kiev, No. 1, 59–65 (2008).
3. G. Weisbrod and D. Rittel, "A Method for Dynamic Fracture Toughness Determination Using Short Beams," Int. J. Fract. **104**, 89–103 (2000).
4. Yu. V. Nemirovskii and T. P. Romanova, "Dynamic Resistance of Plane Plastic Obstacles," (Geo, Novosibirsk, 2009) [in Russian].
5. V. V. Kharchenko, E. A. Kondryakov, and A. V. Panasenko, "Specific Characteristics of Crack Propagation in Steels in Tests with Charpy Samples and Disk Samples," VANT. Kharkov, No. 2 (84), 31–38 (2013).
6. V. R. Bogdanov and G. T. Sulim, "Plain Deformation of Elastoplastic Material with Profile Shaped as a Compact Specimen (Dynamic Loading)," Izv. Akad. Nauk. Mekh. Tverd. Tela, No. 3, 111–120 (2013) [Mech. Solids (Engl. Transl.) **48** (3), 329–336 (2013)].
7. V. R. Bogdanov and G. T. Sulim, "Modeling the Plastic Strain Increase on Impact Based on Numerical Solution of the Plane Stress State Problem," Vestnik MAI **20** (3), 196–201 (2013).
8. V. R. Bogdanov, "Determination of Fracture Viscosity of a Material on the Basis of Numerical Modeling of Plane Deformed State," Vestnik Kiev Nats. Un-tu. Ser. Fiz.-Mat. Nauki, No. 3, 51–56 (2008).
9. V. R. Bogdanov and G. T. Sulim, "Evaluation of Crack Resistance Based on the Numerical Modeling of the Plane Strain State," Fiz. Khim. Mekh. Mater., No. 6, 16–24 (2010) [Mater. Sci. (Engl. Transl.) **46** (6), 723–734 (2011)].
10. V. R. Bogdanov and G. T. Sulim, "Determination of Fracture Viscosity of a Material on the Basis of Numerical Modeling of Three-Dimensional Dynamic Problem," in *Intern. Sci.-Techn. Collection of Papers "Reliability and Durability of Machines and Constructions"*, No. 33, 153-166 (2010).
11. V. R. Bogdanov, "Three-Dimensional Dynamic Problem of Plastic Strain and Stress Concentration near the Crack Tips," Vestnik Kiev Nats. Un-tu. Ser. Fiz.-Mat. Nauki, No. 2, 51–56 (2009).
12. V. V. Piskun and Yu. N. Shevchenko, "Dynamic Elastoplastic Processes of Deformation of Bodies of Rotation under Pulse Loading," in *Actual Aspects of Physical-Mechanical Research* (Naukova Dumka, Kiev, 2007), pp. 239–251.
13. V. I. Makhnenko, "Improvement of Methods for Estimation of Residual Life of Welded Joints in Durable Structures," Avtomatich. Svarka, No. 10–11, 112–121 (2003) [Paton Welding J. (Engl. Transl.), No. 10–11, 107–116 (2003)].
14. B. Z. Margolin, V. A. Shvetsova, A. G. Gulenko, et al., "Fracture Toughness Predictions for a Reactor Pressure Vessel Steel in the Initial and Highly Embrittled States with the Master Curve Approach and a Probabilistic Model," Pressure Vessels and Piping, 219–231 (January 2002).
15. A. G. Gogotsi, "Fracture Toughness Studies on V-Notched Ceramic Specimens," Probl. Prochn. No. 1, 120–127 (2000) [Strength of Materials (Engl. Transl.) **32** (1), 81–85 (2000)].
16. ASTM Standard E399. *Standard Test Method for Plane-Strain Fracture Toughness of Metallic Materials*, in *Annual Book of ASTM Standards*, V.03.1 (ASTM, Philadelphia, PA, 1991).
17. DIN 51 109 *Testing of Advanced Technical Ceramics; Determination of Fracture Toughness (Kic)* (1991).
18. ASTM Standard E1921–97. *Standard Test Method for Determination of Reference Temperature. To the Ferritic Steels in the Transition Range*, in *Annual Book of ASTM Standards*, V.03.1, pp. 1068–1084.
19. US Nuclear Regulatory Commission Guide 1.99 (TASK ME 305-4). *Radiation Embrittlement of Reactor Vessel Materials*, Revision 2, May 1988/
20. M. P. Savruk, *Fracture Mechanics and Strength of Materials*, Vol. 2: *Strain Intensity Factors for Cracked Bodies* (Naukova Dumka, Kiev, 1988) [in Russian].
21. B. Z. Margolin and V. A. Shvetsova, "Brittle Fracture Criterion: Structural Mechanics Approach," Probl. Prochn., No. 2, 3–16 (1992) [Strength of Materials (Engl. Transl.) **24** (2), 115–131 (1992)].
22. E. L. Zyukina, "Conservative Difference Schemes on Uniform Grids for Two-Dimensional Wave Equations," in *Proc. N. I. Lobachevskii Math. Center*, Vol. 26 (Kazan, 2004), pp. 151–160 [in Russian].